

Triangular G^2 -Splines

Hartmut Prautzsch, Georg Umlauf

Abstract. We introduce curvature continuous regular free-form surfaces with triangular control nets. These surfaces are composed of quartic box spline surfaces and are piecewise polynomial multisided patches of total degree 8 which minimize some energy integral. The Bézier nets can be computed efficiently from the spline control net by some fixed masks, i.e. matrix multiplications.

§1. Introduction

Most methods known for building G^k -free-form surfaces need polynomials of relatively high degree, namely $\mathcal{O}(k^2)$, see for example [1,2]. Only recently in 1995 this high degree was beaten by two methods giving G^k -free-form surfaces of bidegree $2k + 2$ with singular [5] and regular [3] parametrizations, respectively. These low degree surfaces can be represented by a control net [3] or a quasi control net [5] and can be designed so as to allow for subdivision.

In this paper we will transfer the method given in [3] to triangular box splines. Here we restrict ourselves to G^2 -surfaces which are the most important for practical applications besides G^1 -surfaces. Further details and the general case are presented in [4,6].

This paper is organized as follows. In paragraph 2 we introduce n -sided G^2 -patches. These patches are used together with generalized C^2 -box spline surfaces to build surfaces of arbitrary topology. How the free parameters in the construction can be used to generate G^2 -splines that minimize certain energy functionals and how these G^2 -splines can be generated efficiently will be discussed in paragraph 3.

§2. P-Patches

The simplest C^2 -box splines are those over the three-directional grid of total polynomial degree four. In this paper we consider only these box splines. A quartic box spline surfaces has a regular triangular control net and each of its polynomial patches is determined by 12 vertices (called control points) which are arranged as in Fig. 1.

Furthermore, we can identify in any triangular net regular subnets of the form of Fig. 1. These subnets determine patches forming a *generalized* box spline surface. A generalized box spline surface has holes corresponding to the

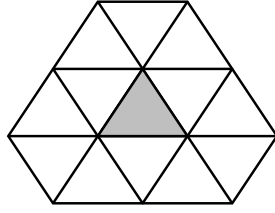


Fig. 1. Schematic illustration of a quartic box spline patch (gray) and its control net.

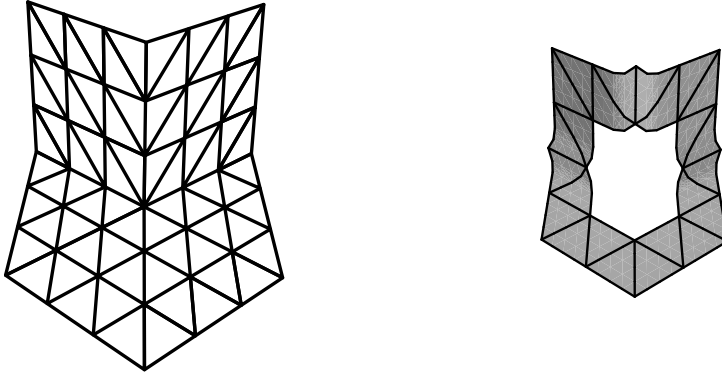


Fig. 2. A triangular net with a vertex of valence 8 (left) and the corresponding generalized quartic box spline surface with an 8-sided hole (right).

irregular vertices in the net. An example is shown in Fig. 2: The control net (left) contains an irregular vertex of valence 8 and the generalized box spline surface (right) has an 8-sided hole.

If every irregular vertex is surrounded by at least three rings of regular vertices, every irregular vertex corresponds to exactly one hole in the generalized quartic box spline surface. In this case an n -sided hole is surrounded by a complete surface ring consisting of $3n$ patches.

How to fill such holes with regular G^2 -surfaces is described in the following:

First for any $n \geq 3, n \neq 6$, we define a special generalized box spline surface that lies in the xy -plane and has the control net shown in Fig. 3 (left) for $n = 5$. Its control points are the points

$$\mathbf{c}_{ijk} := j \begin{bmatrix} c_i \\ s_i \end{bmatrix} + k \begin{bmatrix} c_{i+1} \\ s_{i+1} \end{bmatrix}$$

for $i = 1, \dots, n$ and $j = 0, \dots, 3$ and $k = 0, \dots, 3 - j$, where $c_i = \cos(2\pi i/n)$ and $s_i = \sin(2\pi i/n)$. Thus this surface consists of $3n$ patches, say $\mathbf{x}_{n+1}, \dots, \mathbf{x}_{4n}$, which are shown schematically in Fig. 3 (right).

Second we construct n patches $\mathbf{x}_1, \dots, \mathbf{x}_n$ filling the hole left by the patches $\mathbf{x}_{n+1}, \dots, \mathbf{x}_{4n}$, see Fig. 3 (right). Let

$$\mathbf{x}_l(u, v, w) = \sum \mathbf{b}_{ijk}^l B_{ijk}^4(u, v, w)$$

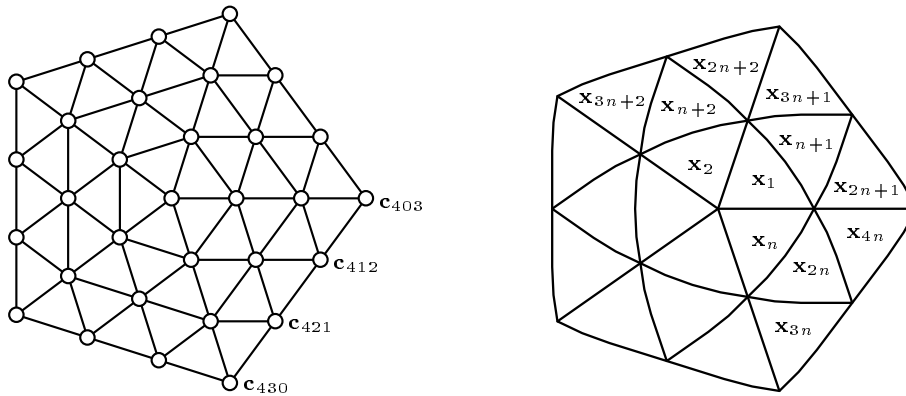


Fig. 3. The control net of $\mathbf{x}_{n+1}, \dots, \mathbf{x}_{4n}$ (left) and the $4n$ planar patches $\mathbf{x}_1, \dots, \mathbf{x}_{4n}$ (right).

be the quartic Bézier representation of the patch x_l , where u, v, w are barycentric coordinates with respect to some reference triangle, i.e. $u \geq 0, v \geq 0, w \geq 0$ and $u + v + w = 1$. The Bézier points of \mathbf{x}_l are determined such that \mathbf{x}_l has C^2 -contact with \mathbf{x}_{n+l} . This fixes, say \mathbf{b}_{ijk}^l , for $i = 0, 1, 2$. Further we set $\mathbf{b}_{400}^l = \mathbf{0}$ and $\mathbf{b}_{3jk}^l = \mathbf{b}_{2,2j,2k}^l/2$. Fig. 4 shows these Bézier points for $n = 5$. Note that the scaling differs from Fig. 3.

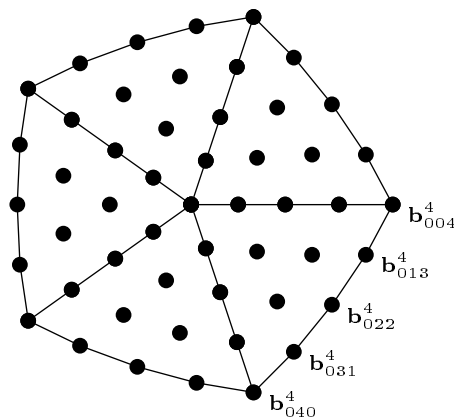


Fig. 4. The Bézier points of $\mathbf{x}_1, \dots, \mathbf{x}_n$ for $n = 5$.

Lemma 1. *The patches $\mathbf{x}_1, \dots, \mathbf{x}_{4n}$ are regular and form a surface without self intersections.*

A proof of this Lemma can be found in [4].

Third for any polynomial $\mathbf{p} : \mathbb{R}^2 \rightarrow \mathbb{R}^3$ we call the union of all patches

$$\mathbf{p}_i(u, v, w) = \mathbf{p}(\mathbf{x}_i(u, v, w)), \quad i = 1, \dots, 4n,$$

a *p-patch*. In the sequel we only consider p-patches of degree (4 or) 8 determined by a (linear or) quadratic polynomial \mathbf{p} . The Bézier points of such a p-patch are illustrated schematically in Fig. 5 for $n = 5$.

Since for $i = n + 1, \dots, 2n$ the patch \mathbf{x}_i has C^2 -contacts with \mathbf{x}_{i-n} , \mathbf{x}_{i+n} and \mathbf{x}_{i+2n} the patch \mathbf{p}_i also has C^2 -contacts with \mathbf{p}_{i-n} , \mathbf{p}_{i+n} and \mathbf{p}_{i+2n} . Similarly, \mathbf{p}_{2n+i} and \mathbf{p}_{3n+i+1} have C^2 -contact for $i = 1, \dots, n$, where $\mathbf{p}_{4n+1} = \mathbf{p}_{3n+1}$. Moreover, since a p-patch is part of a polynomial surface each \mathbf{p}_i , $i = 1, \dots, n$, has G^2 -contact with \mathbf{p}_{i-1} , where $\mathbf{p}_0 := \mathbf{p}_n$.

The Bézier points that define the G^2 -conditions between the patches $\mathbf{p}_1, \dots, \mathbf{p}_n$ are marked by the underlying dark area in Fig. 5. We call them the *G-points* of the p-patch. Leaving these points fixed and changing the other Bézier points arbitrarily such that all C^2 -joints between adjacent \mathbf{p}_i are preserved we obtain a modified p-patch. In general, it does not lie on a polynomial surface, but we will still call such a modified p-patch a *p-patch*.

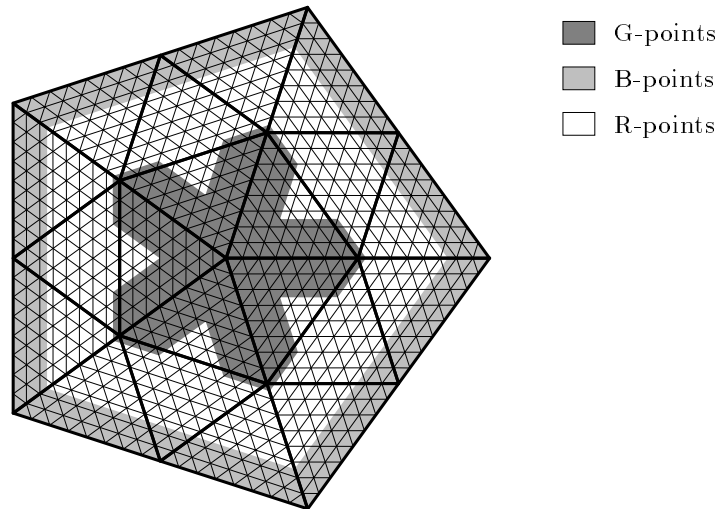


Fig. 5. The Bézier points of a p-patch for $n = 5$.

Theorem 2. Any n -sided hole of a generalized box spline surface can be filled by a p-patch having a C^2 -joint with the generalized box spline surface.

Proof: The boundary and the cross boundary derivatives up to order two of an n -sided p-patch are determined by $45n$ Bézier points. We call these the *B-points* of the p-patch. In Fig. 5 they are marked by the grey area.

The B-points can be changed such that the p-patch fits into an n -sided hole of a generalized box spline surface with a C^2 -contact. The remaining points without the G-points, here called *R-points*, can then be adjusted such that any patch $\mathbf{p}_{n+1}, \dots, \mathbf{p}_{4n}$ of the p-patch has C^2 -contact with all its neighbours. Namely all C^2 -conditions involving R-points form a linear system for the R-points. The matrix of this system is square if we add enough zero rows. After an appropriate permutation of its columns it is even a block-cyclic matrix. This system has an $18n$ parametric solution. Hence there are $18n$ R-points that can be chosen arbitrarily. We call them *A-points*. The other R-points are then determined by the A-,B- and G-points via the C^2 -constraints. We call these the *D-points*.

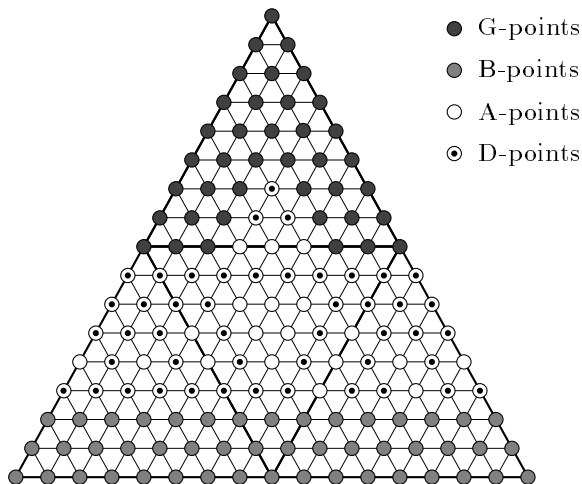


Fig. 6. A possible arrangement of the A-, B-, D- and G-points of $\mathbf{p}_i \cup \mathbf{p}_{i+n} \cup \mathbf{p}_{i+2n} \cup \mathbf{p}_{i+3n}$, $i = 1, \dots, n$.

Fig. 6 shows a possible choice for the A- and D-points. Note that this choice is not unique. \square

§3. Fair p-Patches

The construction of a p-patch that fills a hole of a generalized box spline surface in Theorem 2 is such that different coordinates do not interfere with each other. So, without loss of generality, we restrict ourselves to scalar valued p-patches in the sequel. Thus a point is no longer a point in \mathbb{R}^3 , but in \mathbb{R}^1 .

The G-points of a p-patch are certain Bézier points of a reparametrized quadratic, say

$$q(x, y) = \sum_{i=0}^2 \sum_{j=0}^{2-i} q_{ij} x^i y^j.$$

Hence the G-points depend linearly on the six coefficients q_{ij} , which we call the *Q-points*.

Further, as explained in the proof of Theorem 2 the D-points depend linearly on the A-, B- and G-points. Thus if we consider the B-points fixed, all other Bézier points of the p-patch depend linearly on the six values q_{ij} and the $18n$ A-points.

To obtain good looking surfaces we determine these $6 + 18n$ free parameters such that the p-patch minimizes a quadratic fairness functional. In particular, we have worked with the functional

$$F = \sum_{i=1}^{4n} \int_{\substack{u+v+w=1 \\ u,v,w \geq 0}} \left(\frac{\partial^3}{\partial u^3} \mathbf{p}_i + \frac{\partial^3}{\partial v^3} \mathbf{p}_i + \frac{\partial^3}{\partial w^3} \mathbf{p}_i \right)^2 du dv dw.$$

The D-points of the p-patch depend linearly on the A-, B- and Q-points. So we can view F as a quadratic functional in the A-, B- and Q-points.

Since F is positive definite it is minimal for fixed B-points if its derivatives with respect to the A- and Q-points are zero. Differentiating $F = 0$ with respect to the A- and Q-points leads to equations that are linear in the A-, B- and Q-points. Solving for the A- and Q-points shows that the Bézier points of the p-patch minimizing F depend linearly on the B-points. In other words, there is a matrix M_n depending only on F and n such that $M_n \mathbf{b}$ is the vector of all Bézier points if \mathbf{b} is the vector of all B-points.

Fig. 7 shows an example for the G^2 -p-patch construction. The initial triangular control net has an irregular vertex of valence 5. The isophotes confirm that the resulting surface is G^2 .

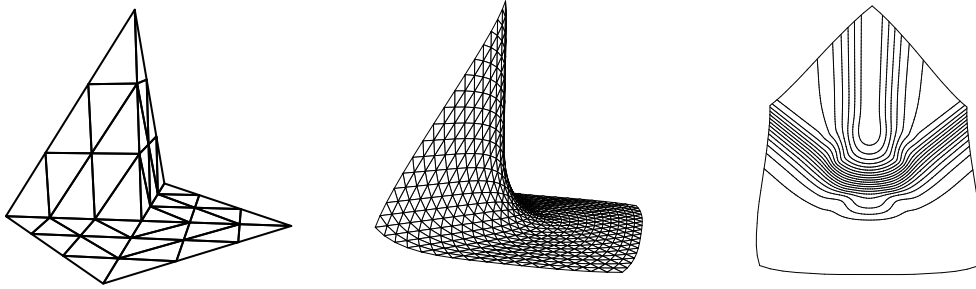


Fig. 7. An initial control net (left), parameter lines of the resulting G^2 -surface (middle), top-view of the surface showing isophotes (right).

Fig. 8 shows a similar example. The control net is the same as in Fig. 7. However, here we used a p-patch consisting of $9n$, $n = 5$, rather than $4n$ patches to fill the n -sided hole of the generalized box spline surfaces.

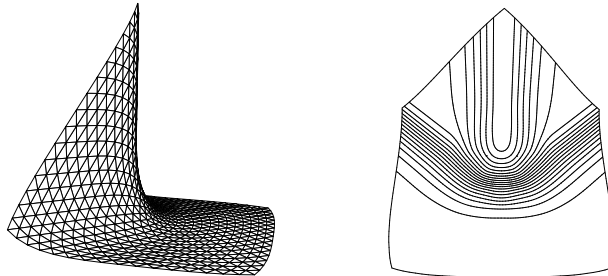


Fig. 8. Parameter lines of the resulting G^2 -surface (left), top-view of the surface showing isophotes (right).

A more complex example is shown in Fig. 9. This G^2 -surface was computed by the same method as Fig. 7.

Remark 3. The matrices M_3, M_4, M_5, M_7, M_8 and M_9 can be found on the website <http://i33www.ira.uka.de>.

Remark 4. The construction above can be generalized for generalized box and half box spline surfaces of smoothness order $2k$ and $2k - 1$, respectively, see [4].

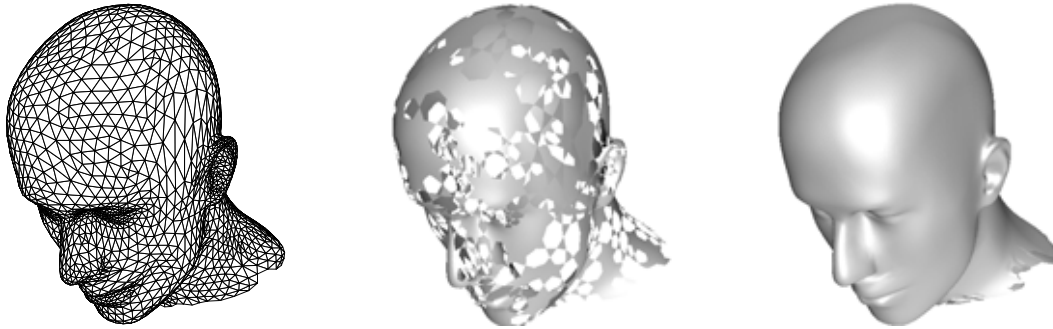


Fig. 9. An initial control net (left), the generalized quartic box spline surface with several holes (middle), the resulting surface where every hole is filled with a p-patch (right).

Acknowledgments. Supported by IWRMM and DFG grant # PR 565/1-1.

References

1. Hahn, J. M., Filling polygonal holes with rectangular patches, in *Theory and Practice in Geometric Modeling*, W. Straßer and H.-P. Seidel (eds.), Springer-Verlag, 1989, 81–91.
2. Mögerle, H., G-Splines höherer Ordnung, PhD thesis, Mathematisches Institut A, Universität Stuttgart, 1992.
3. Prautzsch, H., Freeform splines, *Comput. Aided Geom. Design* **14** (1997), 201–206.
4. Prautzsch, H., and G. Umlauf, Triangular G^k -splines, IWRMM, Universität Karlsruhe, Preprint 99/8, 1999.
5. Reif, U., TURBS – Topologically unrestricted rational B-splines, *Constr. Approx.* **14** (1998), 57–78.
6. Umlauf, G., Glatte Freiformflächen und optimierte Unterteilungsalgorithmen, PhD thesis, IBDS, Universität Karlsruhe, 1999. Verlag Shaker, Aachen.

Hartmut Prautzsch and Georg Umlauf
Institute for Operating- and Dialogsystems
Universität Karlsruhe
D-76128 Karlsruhe
Germany
prau|umlau@ira.uka.de